Published in final edited form as:

Cancer Cell. 2015 April 13; 27(4): 589–602. doi:10.1016/j.ccell.2015.02.016.

Pharmacologic inhibition of the menin-MLL interaction blocks progression of MLL leukemia in vivo

Dmitry Borkin[1,13], **Shihan He**[1,13], **Hongzhi Miao**[1,13], **Katarzyna Kempinska**[1], **Jonathan Pollock**[1,2], **Jennifer Chase**[3,4], **Trupta Purohit**[1], **Bhavna Malik**[1], **Ting Zhao**[5], **Jingya Wang**[1,6], **Bo Wen**[5], **Hongliang Zong**[7], **Morgan Jones**[3,4,8], **Gwenn Danet-Desnoyers**[9], **Monica L. Guzman**[7], **Moshe Talpaz**[10], **Dale L. Bixby**[10], **Duxin Sun**[5], **Jay L. Hess**[1,11], **Andrew G. Muntean**[1], **Ivan Maillard**[3,10,12], **Tomasz Cierpicki**[1], and **Jolanta Grembecka**[1,*]

[1]Department of Pathology, University of Michigan, Ann Arbor, MI, 48109

[2]Graduate Program in Molecular and Cellular Pathology, University of Michigan, Ann Arbor, MI, 48109

[3]Center for Stem Cell Biology, Life Sciences Institute, University of Michigan, Ann Arbor, MI, 48109

[4]Graduate Program in Cellular and Molecular Biology, University of Michigan, Ann Arbor, MI, 48109

[5]College of Pharmacy, University of Michigan, Ann Arbor, MI, 48109

[7]Department of Medicine, Weill Medical College of Cornell University, New York, NY, 10065

[*]Corresponding author: Jolanta Grembecka, PhD, Assistant Professor, Department of Pathology, University of Michigan, 1150 West Medical Center Dr, MSRB I, Room 4510D, Ann Arbor, MI, 48108, jolantag@umich.edu, Tel. 734-615-9319.

[6]Current address: MedImmune, LLC, Gaithersburg, Maryland, MD, 20878

[13]These authors contributed equally to this work

Accession numbers

Microarray data were deposited at the NCBI Gene Expression Omnibus under accession number GSE60673. Crystallography data were deposited at the Protein Data Bank under deposition codes: 4X5Y (menin-MI-503 complex) and 4X5Z (menin-MI-136 complex).

Supplemental Information

Supplemental information includes Supplemental Experimental Procedures, four tables and seven figures.

Conflict of interest

The authors have no relevant conflict of interest.

Author Contributions

D. B. designed and synthesized compounds. S.H, H.M. and K.K. designed and performed animal efficacy studies in MLL leukemia models and biological studies in leukemia cell lines and primary patient samples, J.P. performed crystallography, biochemical and biophysical studies, J.C., M.J. and I.M. designed and performed in vivo experiments to assess the effect of menin-MLL inhibitors on normal hematopoiesis, T.Z., B.W., D.S designed experiments and generated pharmacokinetics and microsomal stability data, J.W. performed bioinformatics analysis of microarray data, T.P. and B.M. performed biochemical and cell biology experiments, H.M., H.Z. and M.G. designed and performed experiments with primary patient samples and interpreted results, G.D-D., M.T., D.B. supported the project with primary patient samples and interpreted data, J.L.H and A.G.M. designed animal studies, interpreted the data and contributed in writing the manuscript, J.G and T.C. directed the entire project, designed the experiments, analyzed the results and wrote the manuscript with the input from all authors.

[8]Medical Scientist Training Program, University of Michigan, Ann Arbor, MI, 48109

[9]Hematology-Oncology, Perelman School of Medicine, University of Pennsylvania, Philadelphia, PA, 19104

[10]Division of Hematology-Oncology, Department of Internal Medicine, University of Michigan, Ann Arbor, MI, 48109

[11]School of Medicine, Indiana University, Indianapolis, IN, 46202

[12]Department of Cell and Developmental Biology, University of Michigan, Ann Arbor, MI, 48109

Summary

Chromosomal translocations affecting Mixed Lineage Leukemia gene (*MLL*) result in acute leukemias resistant to therapy. The leukemogenic activity of MLL fusion proteins is dependent on their interaction with menin, providing basis for therapeutic intervention. Here we report development of highly potent and orally bioavailable small molecule inhibitors of the menin-MLL interaction, MI-463 and MI-503, show their profound effects in MLL leukemia cells and substantial survival benefit in mouse models of MLL leukemia. Finally, we demonstrate efficacy of these compounds in primary samples derived from MLL leukemia patients. Overall, we demonstrate that pharmacologic inhibition of the menin-MLL interaction represents an effective treatment for MLL leukemias in vivo and provide advanced molecular scaffold for clinical lead identification.

Introduction

Acute leukemias represent a paradigm for understanding how genetic and epigenetic modifications lead to tumorigenesis (Figueroa et al., 2010; Rodriguez-Paredes and Esteller, 2011). Despite the complexity of these alterations, which represent a challenge in developing targeted therapies, numerous efforts have been focused on developing effective agents for acute leukemias (Daigle et al., 2011; Dawson et al., 2011; Peloquin et al., 2013; Zuber et al., 2011). Acute leukemias with translocations of the Mixed Lineage Leukemia gene (*MLL*), which constitute about 5–10% of acute leukemias in adults (Marschalek, 2011) and ~70% of acute leukemias in infants (Tomizawa et al., 2007), still represent mostly incurable diseases (Dimartino and Cleary, 1999; Marschalek, 2011). Fusion of *MLL* with one out of over 60 partner genes leads to expression of chimeric MLL fusion proteins, all of which retain an approximately 1,400 amino acids N-terminal fragment of MLL fused with the fusion partner (Hess, 2004; Krivtsov and Armstrong, 2007; Slany, 2009). Expression of MLL fusion proteins enhances proliferation and blocks differentiation of hematopoietic cells, ultimately leading to acute leukemia (Slany, 2005). Patients with MLL leukemias respond poorly to currently available treatments (Slany, 2005), with only about 35% 5-year overall survival rate (Dimartino and Cleary, 1999), emphasizing the urgent need for development of more effective therapies.

The MLL fusion proteins interact with menin, a protein that binds to the N-terminal fragment of MLL retained in all MLL fusion proteins (Caslini et al., 2007; Grembecka et al., 2010; Yokoyama and Cleary, 2008; Yokoyama et al., 2005). Numerous studies

demonstrated a critical role of menin as an oncogenic cofactor in leukemic transformations mediated by MLL fusion proteins (Caslini et al., 2007; Yokoyama and Cleary, 2008; Yokoyama et al., 2005). Menin is a highly specific and direct binding partner of MLL and MLL fusion proteins that is required for regulation of their target genes (Yokoyama et al., 2005). Genetic disruption of the menin-MLL fusion protein interaction abrogates oncogenic properties of MLL fusion proteins and blocks development of acute leukemia in vivo (Yokoyama et al., 2005). These data, together with the evidence that menin is not a requisite cofactor of MLL1 during normal hematopoiesis (Li et al., 2013), validate the menin-MLL interaction as an attractive therapeutic target to develop targeted drugs for MLL leukemia patients.

Despite the critical role of menin in leukemogenesis mediated by MLL fusion proteins, it remains unknown whether pharmacological inhibition of the menin-MLL interaction can suppress development of acute leukemia in vivo and whether it would affect normal hematopoiesis. We previously reported first-generation small molecule inhibitors of the menin-MLL interaction (Grembecka et al., 2012; He et al., 2014; Shi et al., 2012), which represent valuable tool compounds, but are not suitable for in vivo studies due to moderate cellular activity and poor pharmacological properties. The goal of this study was to develop highly potent small molecule inhibitors of the menin-MLL interaction with appropriate pharmacokinetic profile and to determine whether small molecule inhibition of the menin-MLL interaction can represent a valid therapeutic approach for acute leukemias associated with *MLL* rearrangements.

Results

Structure-based development of potent menin-MLL inhibitors

To develop menin-MLL inhibitors with favorable drug-like properties suitable for in vivo efficacy studies, we employed structure-based design and very substantially reengineered our previously reported compounds represented by the most potent MI-2-2, Figure S1A, (Grembecka et al., 2012; Shi et al., 2012). Although MI-2-2 represents a useful chemical tool, it is not suitable for in vivo efficacy studies due to modest cellular activity and very poor metabolic stability (Figure S1A–C). Using the crystal structure of the menin-MI-2-2 complex (Shi et al., 2012) we employed structure-based design combined with medicinal chemistry efforts, resulting in development of menin-MLL inhibitors with modified molecular scaffold (Table S1). These efforts led to identification of MI-136 (Figure 1A), which was developed by introducing the cyano-indole ring connected to the thienopyrimidine core via a piperidine linker (Table S1). MI-136 demonstrates potent inhibitory activity and strong binding affinity to menin (Figure 1A), providing an excellent molecular scaffold for further modifications. Based on the binding mode of MI-136 to menin (Figure S1D), we explored three substitution sites on the indole ring of MI-136 (R1, R2 and R3, Figure 1B) to further improve potency and drug-like properties by optimizing hydrophobic contacts (at R2) or polar interactions (at R1 and R3) (Table S2). The molecular determinants for recognition of MI-136 analogues in the MLL binding site on menin are summarized in Figure 1B. Our medicinal chemistry efforts resulted in identification of two lead compounds: MI-463 and MI-503, which were obtained by combining two (MI-463) or

three (MI-503) best substituents on the indole ring (Figure 1C, Table S2). MI-503 and MI-463 are the most potent inhibitors we developed, both bind to menin with low nanomolar binding affinities, and demonstrate very potent inhibition of the menin-MLL interaction (Figure 1C, 1D and Figure S1E). Crystal structure validates binding of MI-503 to the MLL site on menin (Figure 1E, Table S3). MI-503 occupies the F9 and P13 pockets on menin, forming a hydrogen bond with Tyr276, and also extends beyond the P13 pocket to form hydrogen bonds with Trp341 and Glu366 (Figure 1E). In addition to strong in vitro potency, MI-463 and MI-503 have very favorable drug-like properties, including metabolic stability (Figure S1C) and pharmacokinetic profile in mice (see below), which makes them very attractive candidates to evaluate the therapeutic potential of menin-MLL inhibitors in vivo.

MI-503 and MI-463 demonstrate selective and on-target activity in MLL leukemia cells

We performed a detailed characterization of MI-463 and MI-503 in MLL leukemia cells to assess their activity, selectivity and validate the mechanism of action. First, we found that both compounds can reach the target protein in mammalian cells and effectively inhibit the menin-MLL-AF9 interaction at sub-micromolar concentrations, as assessed in the co-immunoprecipitation experiment (Figure 2A). Treatment of murine bone marrow cells (BMC) transformed with the *MLL-AF9* oncogene with MI-463 and MI-503 resulted in substantial growth inhibition, with half-maximal growth inhibitory concentration (GI_{50}) values of 0.23 μM and 0.22 μM, respectively, measured after 7 days of treatment (Figure 2B). The cell growth inhibitory effect of MI-503 was time-dependent, with a pronounced effect achieved after 7–10 days of treatment (Figure S2A), which is similar to other small molecule inhibitors of epigenetic targets, including DOT1L (Bernt et al., 2011) and EZH2 (Knutson et al., 2012). MI-463 and MI-503 were selective towards MLL-AF9 BMCs as no effect on cell growth inhibition was observed in BMCs transformed with the *Hoxa9/Meis1* oncogenes (HM-2, Figure 2B). Similarly, we observed pronounced growth suppressive activity of MI-503 and MI-463 in a panel of human MLL leukemia cell lines (GI_{50} at 250 nM – 570 nM range for MI-503), but only a minimal effect in human leukemia cell lines without *MLL* translocations (Figure 2C and Figure S2B). Selective killing of MLL leukemia cells is attributed to inhibition of the menin-MLL interaction as the close analogs MI-372 and MI-405, which are much weaker menin-MLL inhibitors (IC_{50} = 0.92 μM and 15.6 μM, respectively), did not show growth suppressive effects in MLL leukemia cells (Figure S2C–S2F).

MI-503 and MI-463 were also very effective in inducing differentiation of MLL leukemia cells, as reflected by pronounced phenotypic changes from primitive blasts to more mature myeloid cells, and substantially increased expression of CD11b, a myeloid differentiation marker (Figure 2D–2F and Figure S2G–S2I). These effects were accompanied by reduced c-kit (CD117) expression, a marker associated with leukemia stem cells (LSCs) (Krivtsov et al., 2006; Somervaille and Cleary, 2006) (Figure S2J–S2K). Interestingly, effects on apoptosis were less pronounced as higher concentrations of both compounds were required for pronounced apoptotic effect in MLL leukemia cells (Figure 2G). Treatment with sub-micromolar concentrations of MI-503 and MI-463 also led to markedly reduced expression of *Hoxa9* and *Meis1*, downstream targets of MLL fusion proteins substantially upregulated in MLL leukemias (Figure 2H). Overall, we developed very potent menin-MLL inhibitors,

which selectively block proliferation of MLL leukemia cells through a specific, on-target mechanism of action, representing very promising candidates for in vivo studies.

To assess the effect of a long-term treatment combined with compound withdrawal we treated MV4;11 human leukemia cells expressing MLL-AF4 with MI-503 followed by the wash-out phase to eliminate the compound and subsequent resupply with MI-503, with each phase continuing for 10 days (Figure 2I and Figure S2L). To avoid cell death, MI-503 was used at 0.2 – 0.6 μM concentrations that inhibit proliferation but do not induce high level apoptosis. As expected, MI-503 induced marked anti-proliferative effects in the first treatment phase, with a GI_{50} value of 200 nM at day 10 (Figure 2I). Withdrawal of MI-503 restored proliferation of MV4;11 cells; however, this effect was concentration-dependent, and less pronounced recovery was observed for cells treated with the highest MI-503 concentration (Figure 2I). Restoration of MI-503 treatment at day 21 resulted in further inhibition of MV4;11 cell proliferation (Figure 2I and Figure S2L). Interestingly, upon prolonged treatment with 0.6 μM of MI-503 the MV4;11 cells began exhausting their proliferative potential (Figure S2L, bottom panel). Furthermore, expression of *HOXA9* and *MEIS1* was markedly reduced at the end of each treatment phase (days 10 and 30), (Figure 2J). In contrast, expression of *HOXA9* and *MEIS1* was restored to the DMSO control level at the end of the wash-out phase (day 20), (Figure 2J). These data support the need for continuous inhibition of menin to block the activity of MLL fusion oncogenes. The ability to suppress proliferation of MV4;11 cells using prolonged treatment with MI-503 suggests that resistance did not develop over the duration of the experiment.

Menin-MLL inhibitors reverse gene expression signatures associated with MLL-rearranged leukemia cells

To assess the effects of menin-MLL inhibitors on global gene expression in the *MLL*-rearranged leukemias, we performed gene expression studies in MV4;11 human leukemia cells (expressing MLL-AF4) after treatment with the MI-389 menin-MLL inhibitor, a close analog of MI-503 with a similar in vitro and cellular activity (Figure S3A–S3B). Significant changes in gene expression were found for 478 and 477 genes up- and downregulated, respectively (Table S4). Gene set enrichment analysis (GSEA) demonstrated strong downregulation of genes identified as downstream targets of MLL-AF4 (Guenther et al., 2008) and MLL-AF9 (Bernt et al., 2011) following treatment with MI-389 (Figure 3A, 3B). These included multiple genes implicated in MLL fusion protein mediated leukemogenesis, such as homeobox genes (*HOXA9*, *HOXA10*, *MEIS1*, *PBX3*), *FLT3* and other downstream targets of MLL fusion proteins *(MEF2C*, *BCL2* and *CDK6)* (Figure 3A, 3B and Table S4). Downregulated expression of these genes was consistent with phenotypic consequences of treatment with the menin-MLL inhibitor (Figure S3C). GSEA also revealed a global upregulation of genes underexpressed in leukemia stem cells ($CD34^+$ $CD38^-$ progenitor cells) (Gal et al., 2006) and in primitive hematopoietic progenitor cells (Jaatinen et al., 2006), including genes associated with differentiation (*ITGAM*, which encodes the cell surface marker CD11b associated with myeloid differentiation, and *MNDA*), following MI-389 treatment, Figure 3C.

We have further used qRT-PCR to validate expression changes for selected genes in MV4;11 and MOLM-13 (expressing MLL-AF9) human leukemia cell lines upon treatment with MI-389 and MI-503 (Figure 3D, 3E). We observed markedly downregulated expression of Homeobox genes (*HOXA9*, *HOXA10*, *HOXA7*, *PBX3*, *MEIS1*) and other downstream targets of MLL fusion proteins (*DLX2*, *MEF2C*, *FLT3*) and up-regulation of *MNDA*, a differentiation marker of myeloid cells (Figure 3D, 3E), consistent with the gene expression data from the microarray studies in MV4;11 cells (Figure 3A, 3B). Overall, these results demonstrate that pharmacologic inhibition of the menin-MLL interaction reverses the gene expression signature in *MLL*-rearranged leukemia cells, providing an attractive strategy to reprogram these cells towards differentiation.

Menin-MLL inhibitors block hematologic tumors in vivo and reduce MLL leukemia tumor burden

We next aimed to establish the therapeutic potential of menin-MLL inhibitors in vivo using mouse models of MLL leukemia. First, we characterized the pharmacokinetic (PK) properties of MI-503 and MI-463 in mice. Both compounds achieved high level in peripheral blood following a single intravenous or oral dose, while also showing high oral bioavailability (~45% for MI-463 and 75% for MI-503), Figure 4A and Figure S4A. We then assessed the effect of MI-463 and MI-503 on in vivo tumor growth in mouse xenograft model utilizing MV4;11 human MLL leukemia cells implanted into BALB/c nude mice. Both MI-463 and MI-503 induced strong inhibition of tumor growth with once daily intraperitoneal (i.p.) administration, albeit MI-503 showed more pronounced effects (Figure 4B). Treatment with MI-503 resulted in an over 80% reduction in MV4;11 tumor volume and complete tumor regression in two mice. Pronounced tumor growth inhibition correlated well with the level of both compounds in the tumor samples (Figure S4B). Importantly, prolonged treatment (38 days) with MI-503 induced no toxicity in mice as reflected by no alterations in the body weight and no morphological changes in liver and kidney tissues (Figure S4C, S4D). Furthermore, gene expression studies performed in samples isolated from the MV4;11 tumors revealed significant reduction in expression of MLL fusion protein target genes, *HOXA9* and *MEIS1*, upon treatment with MI-503 and MI-463 (Figure 4C). Taken together, the reduction in tumor growth correlated with a decrease in expression of MLL-fusion target genes in vivo, validating on-target activities of MI-463 and MI-503.

We then assessed the effect of MI-503 and MI-463 in disseminated human MLL-AF4 leukemia using a xenotransplantation model. MV4;11 cells expressing luciferase were injected into NSGS or NSG mice via tail vein and treatment was initiated 5 days later to allow for efficient engraftment of leukemic cells. Leukemia progression was monitored by bioluminescence imaging. Based on the pharmacokinetic profiles, we selected twice-daily treatment regimen to sustain a therapeutic concentration of the compounds in the blood. Ten consecutive days of treatment with MI-503 resulted in a marked delay in progression of MLL leukemia in mice and significantly reduced leukemia tumor burden (Figure 4D and Figure S4E). Similarly, 20 days treatment of MV4;11 xenograft recipient mice with MI-463 also resulted in a substantial delay in leukemia progression as manifested by a marked decrease in the bioluminescence level measured over the course of the experiment (Figure 4E, 4F). Reduced bioluminescence was associated with a significant decrease in the

population of leukemic cells in the peripheral blood, spleen and bone marrow samples harvested from mice treated with MI-463 (Figure 4G). Furthermore, we observed reduced expression of MLL fusion target genes (*HOXA9*, *MEIS1*, *MEF2C*) and increase in the expression level of *ITGAM* upon treatment of mice with MI-463 (Figure 4H). Collectively, these findings demonstrate that MI-503 and MI-463 have a potent anti-leukemic effect in vivo when applied as single agents. Importantly, these data suggest that resistance did not emerge after prolonged (20 days) treatment with MI-463.

Menin-MLL inhibitors substantially improve survival of MLL leukemic mice

We next assessed the effects of menin-MLL inhibitors on survival of MLL leukemia mice, using a bone marrow transplantation model of murine MLL-AF9 leukemia (Figure S5A). Despite short latency time in this aggressive leukemia model (~15 days) we initiated treatment five days after transplantation to test efficacy of menin-MLL inhibitors in the established disease model. MI-463 at 50 mg/kg and MI-503 at 80 mg/kg were administered twice daily by oral gavage for ten consecutive days. The presence of abundant blasts in the peripheral blood, bone marrow and spleen was used to validate terminal leukemia in mice (Figure S5B). Importantly, treatment with either compound strongly delayed leukemia progression as reflected by a substantial survival benefit in MLL-AF9 leukemia mice when MI-463 and MI-503 were applied as single agents (Figure 5A). The median survival of MLL-AF9 leukemia mice was increased by ~70% and ~45% upon treatment with MI-463 and MI-503, respectively (Figure 5A), demonstrating their pronounced effects in blocking MLL leukemia progression in vivo.

To further validate that treatment with menin-MLL inhibitors delayed leukemia progression, we additionally tested the MI-463 compound in the MLL-AF9 leukemia model using the same treatment regimen as in survival experiment (Figure 5A). Following 10 days of treatment all animals were sacrificed and extensive analysis of leukemia progression was performed in vehicle and compound treated cohorts with samples collected at the same time point. We observed notably reduced spleen size and weight (Figure 5B and 5C) and substantially decreased level of blasts in bone marrow samples upon treatment with MI-463 versus vehicle control (Figure 5D and 5E). These effects were accompanied by substantially reduced blast infiltration of the liver and spleen upon treatment with MI-463 (Figure 5F and Figure S5C). The bone marrow samples isolated from mice treated with MI-463 showed a sub-population of cells with a differentiated phenotype as manifested by the appearance of cells with a neutrophil-like morphology (Figure 5G). The white blood cell count was decreased in the peripheral blood of the MLL-AF9 mice upon treatment with MI-463, while other blood cells and blood parameters were not affected (Figure 5H and Figure S5D). MI-463 administration was well tolerated, and no significant body weight loss was observed (Figure S5E). Furthermore, treatment of mice with MI-463 resulted in a marked reduction in the expression level of MLL-fusion downstream targets, *Hox9*, *Meis1*, *Mef2c* and *Flt3*, as well as a substantial increase in the expression level of *Itgam* differentiation marker in the bone marrow samples (Figure 5I). Taken together, these data demonstrate that pharmacologic inhibition of the menin-MLL interaction substantially delays progression of MLL leukemia in vivo in murine models through on-target activity without causing toxicity.

Menin-MLL inhibitors do not impair normal hematopoiesis in vivo

Given the role of MLL1 in normal hematopoiesis (Ernst et al., 2002; McMahon et al., 2007), we assessed whether pharmacological inhibition of the menin-MLL interaction affects the normal hematopoiesis in mice. C57BL/6 mice were treated with efficacious doses of MI-463 and MI-503 for 10 days using the same treatment regimen as in survival experiments (Figure 5A). Importantly, no decrease in body weight, organ weight or tissue damage was observed upon treatment with either compound (Figure S6A–S6C). We then performed detailed analysis of bone marrow samples and found that bone marrow cellularity was preserved upon treatment with MI-463 and MI-503 (Figure 6A). Flow cytometric analysis showed that bone marrow cell populations highly enriched for hematopoietic stem cells were not decreased upon treatment with menin-MLL inhibitors (LSK progenitors defined as $Lin^{-}Sca\text{-}1^{+}c\text{-}Kit^{+}$ and long-term hematopoietic stem cells defined as LSK $CD48^{-}CD150^{+}$) (Figure 6B). In fact these populations were even slightly increased upon treatment. Analysis of mature myeloid cells ($CD11b^{+}Gr\text{-}1^{+}$) showed no impact in the inhibitor-treated mice (Figure 6C). Phenotypic analysis of B cell populations showed a mild increase in pro-B cell numbers and no effect on other B cells populations upon treatment with MI-463 and MI-503 (Figure 6D and Figure S6D). Gene expression analysis performed in LSK progenitors showed no reduction in the expression level of the menin and/or MLL dependent genes, including *Hoxa9* and *Meis1*, upon treatment of mice with MI-463 or MI-503 (Figure 6E and Figure S6E). This is consistent with the modest effect on expression of these genes reported in LSKs after genetic loss of *Men1* encoding menin (Artinger et al., 2013; Li et al., 2013; Maillard et al., 2009). These results suggest that the MLL-rearranged cells are more sensitive to the treatment with the menin-MLL inhibitors than normal LSKs, supporting the existence of a therapeutic window for these compounds.

We have also assessed the effect of MI-503 on normal hematopoiesis after prolonged treatment of mice (38 days of continued treatment with efficacious doses of MI-503) using the xenograft MV4;11 model described above (Figure 4B). No significant effect on bone marrow cellularity, $Lin^{-}c\text{-}Kit^{+}$ progenitors and long-term hematopoietic stem cells was observed (Figure 6F–6G), with a slight increase in mature myeloid cells in bone marrow (Figure 6F). Overall, these findings show that pharmacologic inhibition of the menin-MLL interaction dose not negatively affect normal hematopoiesis, which rules out a potential “on-target” toxicity of the menin-MLL inhibitors. Importantly, our results are in agreement with recent studies suggesting that menin is not a requisite cofactor of MLL1 during normal hematopoiesis (Li et al., 2013; Maillard and Hess, 2009).

Menin-MLL inhibitors selectively kill MLL leukemia primary patient samples

To evaluate therapeutic potential of menin-MLL inhibitors we studied the effects of MI-503 and MI-463 on primary samples isolated from MLL leukemia patients as well as in several AML patient samples without *MLL* translocation (Figure S7A, S7B). Both compounds substantially reduced clonogenic efficiency in all MLL leukemia patient samples, with over 50% reduction in colony number at submicromolar or low micromolar concentrations (Figure 7A). Notably, the morphology and size of colonies changed upon treatment with menin-MLL inhibitors, resulting in significantly smaller and more diffuse colonies when compared to DMSO treated samples (Figure 7C). In contrast, both compounds had little

effect on colony formation in control AML patient samples, except at the highest concentration (6 μM) in the AML-9571 sample (Figure 7B and 7C).

We also assessed the effect of MI-463 in an additional set of AML patient samples and observed a marked decrease in cell growth and blast population in MLL leukemia patient samples but not in primary AML samples without *MLL* translocations (Figure 7D, 7E and Figure S7C–S7D). Furthermore, increased cell size was observed following treatment with MI-463 specifically in primary MLL leukemia cells but not in other AML samples (Figure 7E), suggesting differentiation of these cells, although this effect needs further investigation. No effect on growth and blast population in the primary MLL patient samples was detected for MI-372 negative control compound (Figure S7C–S7E). Taken together, these data provide compelling evidence supporting the therapeutic potential of menin-MLL inhibitors in MLL leukemias.

Discussion

Acute leukemias with *MLL* rearrangements represent an unmet medical need as therapeutic agents have not been developed for clinical use in MLL leukemia patients. Menin plays a critical role as an oncogenic co-factor of MLL fusion proteins in leukemia (Yokoyama et al., 2005). Based on genetic data, inhibition of the menin-MLL interaction was proposed as a potential therapeutic approach (Li et al., 2013; Yokoyama et al., 2005), but this strategy has not been validated with pharmacologic agents. Here, we demonstrate that pharmacologic inhibition of the menin-MLL interaction with small molecules blocks progression of MLL leukemia in vivo without impairing normal hematopoiesis. These effects were achieved with small molecule inhibitors MI-463 and MI-503 that directly bind to menin with low nanomolar binding affinities and effectively block the menin-MLL interaction. Both compounds have appropriate pharmacokinetic profile and high oral bioavailability and their in vivo administration results in a substantial extension of survival in a mouse model of MLL leukemia through on-target mechanism of action. Importantly, these compounds do not impair normal hematopoiesis in mice, providing evidence that a sufficient therapeutic window can be achieved. Overall, this study supports clinical applications of menin-MLL inhibitors as targeted therapeutics against *MLL*-rearranged leukemias.

Based on our studies, MI-463 and MI-503 are two lead compounds with comparable efficacy and drug-like properties. MI-503 has better oral bioavailability and can be tolerated at higher doses in mice, but at this point we cannot distinguish which compound might represent a better candidate for further development as targeted therapy for the treatment of patients suffering from MLL leukemia. Follow-up studies, including pharmacological formulation, pharmacokinetic studies and long term toxicity in other species, including rats and dogs, are required to address this question. In case any potential undesired side effects emerge, additional substitutions on the indole ring of MI-463 or MI-503 could be explored to modulate these properties.

In this study we provide an example of targeted drug discovery where the oncogenic effects of genetic alterations can be reversed by effective blocking of a protein-protein interaction critical for oncogenesis. This approach represents an attractive strategy to develop therapies,

as protein-protein interactions typically show a high level of evolutionary conservation and functional mutations leading to drug resistance are far less likely to occur than in enzymes. These considerations, together with the results of our studies, validate that in vivo pharmacological inhibition of the menin-MLL fusion protein interaction offers a promising therapeutic opportunity for acute leukemias with *MLL* rearrangements. Recent reports emphasize oncogenic role of menin in other cancers, including hepatocellular carcinomas (Xu et al., 2013), raising a possibility that pharmacologic inhibition of this protein-protein interaction might have broader therapeutic applications in oncology, both for hematologic malignancies and solid tumors. The two compounds we report here may represent clinical lead candidates or provide an advanced molecular scaffold for further optimization into clinical lead compounds.

Experimental Procedures

Chemistry

Chemical synthesis and chemical characterization of compounds are provided in the Supplemental Experimental Procedures.

Biochemical, biophysical and structural characterization of menin-MLL inhibitors

Inhibition of the menin-MLL interaction by small molecules was assessed by fluorescence polarization (FP) assay using the protocol described previously (Grembecka et al., 2010; Grembecka et al., 2012). Binding affinity of compounds (MI-136, MI-389, MI-463 and MI-503) to menin was assessed using Isothermal Titration Calorimetry experiments performed at 25 °C with compounds (50 μM – 100 μM) injected into menin (5 μM – 10 μM) in 10 μl aliquots. For co-crystallization experiments 2.5 mg/mL menin was incubated with small molecule inhibitors (MI-136 or MI-503) at 1:3 molar ratio. Crystals were obtained using the sitting drop technique at 10 °C by applying the procedure described previously (Shi et al., 2012). More details can be obtained in Supplemental Experimental Procedures.

Viability assays, cell differentiation and gene expression studies

For viability assays, leukemia cells were plated at relevant concentrations and treated with compounds or 0.25% DMSO and cultured at 37 °C for 7 days. Media was changed at day 4, viable cell numbers were restored to the original concentration and compounds were re-supplied. MTT cell proliferation assay kit (Roche) was then employed, and plates were read for absorbance at 570 nm using a PHERAstar BMG microplate reader. Effect of menin-MLL inhibitors on expression level was assessed by Real-time quantitative PCR (qRT-PCR) after 6 days of incubation of compounds with cells, with media changed and compound re-supply at day 3. For cell differentiation studies, leukemia cells were treated with menin-MLL inhibitors for 7 days, then harvested, washed and incubated with Pacific Blue rat anti-mouse CD11b antibody (BD BioLegend, cat # 101224) before being analyzed by flow cytometry. More details can be obtained in Supplemental Experimental Procedures.

Efficacy studies in mice

All animal experiments were approved by the University of Michigan Committee on Use and Care of Animals and Unit for Laboratory Animal Medicine (ULAM). For efficacy

studies in MV4;11 subcutaneous xenograft mice model, 5×10^6 cells were injected into the 4–6 week old female BALB/c nude mice. Treatment was started when the tumor size reached ~100 mm^3. Vehicle (25% DMSO, 25% PEG400, 50% PBS) or compounds (MI-463 or MI-503) were administrated once daily at designated doses using i.p. injections. For mice efficacy studies in bioimaging MV4;11 xenograft model, 6 to 8-week-old female NSGS or NSG mice were intravenously injected with 1×10^7 or 0.5×10^7 luciferase-expressing MV4;11 cells. At day 5, treatment with compound of vehicle was initiated and continued for 10–20 consecutive days. To generate the MLL-AF9 leukemic mice, C57BL/6 female mice were transplanted with 1×10^5 spleen or bone marrow cells isolated from the primary recipient mice. Five days post-transplantation treatment with MI-463, MI-503 or vehicle was initiated and continued for 10 days. Mice were sacrificed upon signs of disease. Leukemia was confirmed by flow cytometric analysis of GFP^+ cells as a surrogate for MLL-AF9 expression. More details can be obtained in Supplemental Experimental Procedures.

Analysis of normal hematopoiesis in mice

Normal hematopoiesis was studies in C57BL/6 mice after 10 days of treatment with MI-463, MI-503 or vehicle control and in the BALB/c nude mice after 38 days of treatment with MI-503. See Supplemental Experimental Procedures for more details.

Primary patient samples

Patient-derived AML samples were collected in accordance with the guidelines and approval of institutional review boards at University of Pennsylvania Hospital, Weill Cornell Medical College, New York Presbyterian Hospital, and University of Michigan Hospital, and informed consent of each patient. Peripheral blood samples were collected and processed to isolate mononuclear cells using density gradient centrifugation and red blood cell lysis. Cells were frozen in 10% DMSO until used in experiments.

Clonogenic assay in methylcellulose with primary patient samples

Primary patient samples were grown in RPMI-1640 media (Lifetechnologies), supplemented with 10% FBS and 1% penicillin/streptomycin, in the presence of 10 ng/mL human IL-3, 10 ng/mL IL-6 and 50 ng/m LSCF (PeproTech). 24 hr later, cells were plated in duplicates on methylcellulose media supplemented with human cytokines (Methocult H4435, StemCell Technologies) with cell density of $7.5–15 \times 10^4$ cells. Compounds or DMSO were added to the methylcellulose and incubated at 37 °C, 5% CO_2 for 14 days at which time colonies were stained with iodonitrotetrazolium chloride and counted.

Cell viability assay in primary patient samples

Primary AML samples were treated with the compounds or vehicle (0.25% DMSO) for 7 days. Cells were collected and stained with mouse anti-human CD45-APC-H7 (BD Bioscience), CD34-APC and CD38-PE-Cy7 (eBiosciences) prior to Annexin V (BD Bioscience) and 7-AAD (Life Technologies) staining. Cells were then analyzed using an LSR II flow cytometer (BD Bioscience) collecting at least 2×10^5 events for each sample. Data analysis was performed using FlowJo 9.3.2 software for Mac OS X (TreeStar).

Annexin V and 7-AAD double negative cells were scored as viable, and the viability was represented as the percent relative to DMSO treated cells.

Statistical analysis

Student's t-test (unpaired, two-tailed) was used to calculate significance level between treatment groups in all experiments besides survival curves, where Log-rank (Mantel-Cox) test was applied to calculate p values. P values of less than 0.05 were considered significant. Graph generation and statistical analysis were performed using GraphPad Prism version 6.02 software (GraphPad, La Jolla, CA).

Supplementary Material

Refer to Web version on PubMed Central for supplementary material.

Acknowledgments

The authors acknowledge Dr. Arul Chinnaiyan for critical reading of this manuscript and fruitful discussion. We thank Dr. Moshe Talpaz and Malathi Kandarpa for access to primary patient samples from Hematological Malignancies Tissue Repositories, University of Michigan and Dr. Gwenn Danet-Desnoyers from Stem Cell and Xenograft Core at the University of Pennsylvania, for providing additional set of patient samples. We thank Dr. Thomas Look, Dana Farber Cancer Institute, for providing MV4;11 cells expressing luciferase. MV4;11 cells for subcutaneous xenograft studies were purchased from ATCC. We thank Dr. John Bushweller for providing human leukemia cell lines for this project. This work was funded by the National Institute of Health (NIH) grant R01 (1R01CA160467) to J.G., NIH T32 (HD007505 and GM007315) to J.C., a Leukemia and Lymphoma Society (LLS) TRP grant (6116-12) to J.G., LLS Scholar (1215-14) to J.G., LLS TAP (Therapy Acceleration Program) to J.G., American Cancer Society grants (RSG-11-082-01-DMC to T.C. and RSG-13-130-01-CDD to J.G.), and the Department of Pathology, University of Michigan. Use of the Advanced Photon Source was supported by the US Department of Energy, Office of Science, Office of Basic Energy Sciences under contract number DE-AC02-06CH11357. Use of the LS-CAT Sector 21 was supported by the Michigan Economic Development Corporation and the Michigan Technology Tri-Corridor for the support of this research program (grant 085P1000817). The mouse work was performed under oversight of UCUCA at the University of Michigan.

References

Artinger EL, Mishra BP, Zaffuto KM, Li BE, Chung EK, Moore AW, Chen Y, Cheng C, Ernst P. An MLL-dependent network sustains hematopoiesis. Proc Natl Acad Sci U S A. 2013; 110:12000–12005. [PubMed: 23744037]

Bernt KM, Zhu N, Sinha AU, Vempati S, Faber J, Krivtsov AV, Feng Z, Punt N, Daigle A, Bullinger L, et al. MLL-rearranged leukemia is dependent on aberrant H3K79 methylation by DOT1L. Cancer Cell. 2011; 20:66–78. [PubMed: 21741597]

Caslini C, Yang Z, El-Osta M, Milne TA, Slany RK, Hess JL. Interaction of MLL amino terminal sequences with menin is required for transformation. Cancer Res. 2007; 67:7275–7283. [PubMed: 17671196]

Daigle SR, Olhava EJ, Therkelsen CA, Majer CR, Sneeringer CJ, Song J, Johnston LD, Scott MP, Smith JJ, Xiao Y, et al. Selective killing of mixed lineage leukemia cells by a potent small-molecule DOT1L inhibitor. Cancer Cell. 2011; 20:53–65. [PubMed: 21741596]

Dawson MA, Prinjha RK, Dittmann A, Giotopoulos G, Bantscheff M, Chan WI, Robson SC, Chung CW, Hopf C, Savitski MM, et al. Inhibition of BET recruitment to chromatin as an effective treatment for MLL-fusion leukaemia. Nature. 2011; 478:529–533. [PubMed: 21964340]

Dimartino JF, Cleary ML. Mll rearrangements in haematological malignancies: lessons from clinical and biological studies. Br J Haematol. 1999; 106:614–626. [PubMed: 10468849]

Ernst P, Wang J, Korsmeyer SJ. The role of MLL in hematopoiesis and leukemia. Curr Opin Hematol. 2002; 9:282–287. [PubMed: 12042701]

Figueroa ME, Lugthart S, Li Y, Erpelinck-Verschueren C, Deng X, Christos PJ, Schifano E, Booth J, van Putten W, Skrabanek L, et al. DNA methylation signatures identify biologically distinct subtypes in acute myeloid leukemia. Cancer Cell. 2010; 17:13–27. [PubMed: 20060365]

Gal H, Amariglio N, Trakhtenbrot L, Jacob-Hirsh J, Margalit O, Avigdor A, Nagler A, Tavor S, Ein-Dor L, Lapidot T, et al. Gene expression profiles of AML derived stem cells; similarity to hematopoietic stem cells. Leukemia. 2006; 20:2147–2154. [PubMed: 17039238]

Grembecka J, Belcher AM, Hartley T, Cierpicki T. Molecular basis of the mixed lineage leukemia-menin interaction: implications for targeting mixed lineage leukemias. J Biol Chem. 2010; 285:40690–40698. [PubMed: 20961854]

Grembecka J, He S, Shi A, Purohit T, Muntean AG, Sorenson RJ, Showalter HD, Murai MJ, Belcher AM, Hartley T, et al. Menin-MLL inhibitors reverse oncogenic activity of MLL fusion proteins in leukemia. Nat Chem Biol. 2012; 8:277–284. [PubMed: 22286128]

Guenther MG, Lawton LN, Rozovskaia T, Frampton GM, Levine SS, Volkert TL, Croce CM, Nakamura T, Canaani E, Young RA. Aberrant chromatin at genes encoding stem cell regulators in human mixed-lineage leukemia. Genes Dev. 2008; 22:3403–3408. [PubMed: 19141473]

He S, Senter TJ, Pollock J, Han C, Upadhyay SK, Purohit T, Gogliotti RD, Lindsley CW, Cierpicki T, Stauffer SR, Grembecka J. High-affinity small-molecule inhibitors of the menin-mixed lineage leukemia (MLL) interaction closely mimic a natural protein-protein interaction. J Med Chem. 2014; 57:1543–1556. [PubMed: 24472025]

Hess JL. MLL: a histone methyltransferase disrupted in leukemia. Trends Mol Med. 2004; 10:500–507. [PubMed: 15464450]

Jaatinen T, Hemmoranta H, Hautaniemi S, Niemi J, Nicorici D, Laine J, Yli-Harja O, Partanen J. Global gene expression profile of human cord blood-derived CD133+ cells. Stem Cells. 2006; 24:631–641. [PubMed: 16210406]

Knutson SK, Wigle TJ, Warholic NM, Sneeringer CJ, Allain CJ, Klaus CR, Sacks JD, Raimondi A, Majer CR, Song J, et al. A selective inhibitor of EZH2 blocks H3K27 methylation and kills mutant lymphoma cells. Nat Chem Biol. 2012; 8:890–896. [PubMed: 23023262]

Krivtsov AV, Armstrong SA. MLL translocations, histone modifications and leukaemia stem-cell development. Nat Rev Cancer. 2007; 7:823–833. [PubMed: 17957188]

Krivtsov AV, Twomey D, Feng Z, Stubbs MC, Wang Y, Faber J, Levine JE, Wang J, Hahn WC, Gilliland DG, et al. Transformation from committed progenitor to leukaemia stem cell initiated by MLL-AF9. Nature. 2006; 442:818–822. [PubMed: 16862118]

Li BE, Gan T, Meyerson M, Rabbitts TH, Ernst P. Distinct pathways regulated by menin and by MLL1 in hematopoietic stem cells and developing B cells. Blood. 2013; 122:2039–2046. [PubMed: 23908472]

Maillard I, Chen YX, Friedman A, Yang Y, Tubbs AT, Shestova O, Pear WS, Hua X. Menin regulates the function of hematopoietic stem cells and lymphoid progenitors. Blood. 2009; 113:1661–1669. [PubMed: 19228930]

Maillard I, Hess JL. The role of menin in hematopoiesis. Adv Exp Med Biol. 2009; 668:51–57. [PubMed: 20175452]

Marschalek R. Mechanisms of leukemogenesis by MLL fusion proteins. Br J Haematol. 2011; 152:141–154. [PubMed: 21118195]

McMahon KA, Hiew SY, Hadjur S, Veiga-Fernandes H, Menzel U, Price AJ, Kioussis D, Williams O, Brady HJ. Mll has a critical role in fetal and adult hematopoietic stem cell self-renewal. Cell Stem Cell. 2007; 1:338–345. [PubMed: 18371367]

Peloquin GL, Chen YB, Fathi AT. The evolving landscape in the therapy of acute myeloid leukemia. Protein Cell. 2013; 4:735–746. [PubMed: 23982740]

Rodriguez-Paredes M, Esteller M. Cancer epigenetics reaches mainstream oncology. Nat Med. 2011; 17:330–339. [PubMed: 21386836]

Shi A, Murai MJ, He S, Lund G, Hartley T, Purohit T, Reddy G, Chruszcz M, Grembecka J, Cierpicki T. Structural insights into inhibition of the bivalent menin-MLL interaction by small molecules in leukemia. Blood. 2012; 120:4461–4469. [PubMed: 22936661]

Slany RK. When epigenetics kills: MLL fusion proteins in leukemia. Hematol Oncol. 2005; 23:1–9. [PubMed: 16118769]

Slany RK. The molecular biology of mixed lineage leukemia. Haematologica. 2009; 94:984–993. [PubMed: 19535349]

Somervaille TC, Cleary ML. Identification and characterization of leukemia stem cells in murine MLL-AF9 acute myeloid leukemia. Cancer Cell. 2006; 10:257–268. [PubMed: 17045204]

Tomizawa D, Koh K, Sato T, Kinukawa N, Morimoto A, Isoyama K, Kosaka Y, Oda T, Oda M, Hayashi Y, et al. Outcome of risk-based therapy for infant acute lymphoblastic leukemia with or without an MLL gene rearrangement, with emphasis on late effects: a final report of two consecutive studies, MLL96 and MLL98, of the Japan Infant Leukemia Study Group. Leukemia. 2007; 21:2258–2263. [PubMed: 17690691]

Xu B, Li SH, Zheng R, Gao SB, Ding LH, Yin ZY, Lin X, Feng ZJ, Zhang S, Wang XM, Jin GH. Menin promotes hepatocellular carcinogenesis and epigenetically up-regulates Yap1 transcription. Proc Natl Acad Sci U S A. 2013; 110:17480–17485. [PubMed: 24101467]

Yokoyama A, Cleary ML. Menin critically links MLL proteins with LEDGF on cancer-associated target genes. Cancer Cell. 2008; 14:36–46. [PubMed: 18598942]

Yokoyama A, Somervaille TC, Smith KS, Rozenblatt-Rosen O, Meyerson M, Cleary ML. The menin tumor suppressor protein is an essential oncogenic cofactor for MLL-associated leukemogenesis. Cell. 2005; 123:207–218. [PubMed: 16239140]

Zuber J, Shi J, Wang E, Rappaport AR, Herrmann H, Sison EA, Magoon D, Qi J, Blatt K, Wunderlich M, et al. RNAi screen identifies Brd4 as a therapeutic target in acute myeloid leukaemia. Nature. 2011; 478:524–528. [PubMed: 21814200]

Significance

Chromosomal translocations of *MLL* occur in aggressive acute leukemias affecting both children and adults. MLL fusion proteins require menin for leukemogenic activity, and selective targeting of the menin-MLL interaction represents a potential therapeutic approach for acute leukemias with *MLL* rearrangements. Here, we report development of very potent and orally bioavailable small molecule inhibitors of the menin-MLL interaction, MI-463 and MI-503, which effectively block progression of MLL leukemia in vitro and in vivo, without affecting normal hematopoiesis. We also demonstrate efficacy of these compounds in primary leukemia samples derived from MLL leukemia patients. These studies provide a rationale for clinical evaluation of the menin-MLL inhibitors as a valuable therapeutic approach for acute leukemias associated with *MLL* rearrangements.

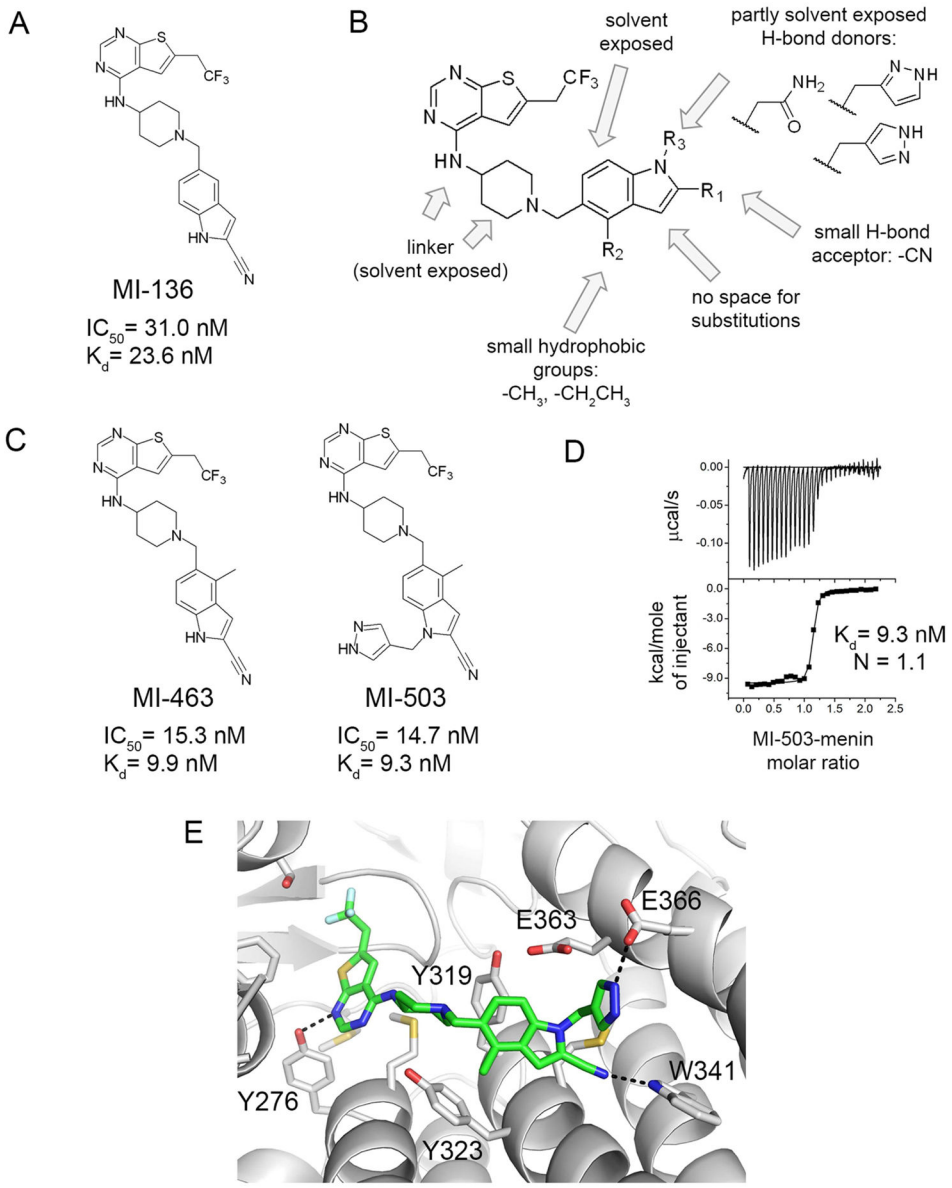

Figure 1. Structure-based development of potent menin-MLL inhibitors

(A) Chemical structure and in vitro activity for MI-136. IC_{50} was measured by fluorescence polarization assay and K_d was determined by Isothermal Titration Calorimetry (ITC). (B) Summary of structure-activity relationship for menin-MLL inhibitors. R1, R2 and R3 indicate substitution sites explored for modifications. Best substituents at R1, R2 and R3 positions are shown. (C) Structures and activities of MI-463 and MI-503 menin-MLL inhibitors. (D) Binding isotherm from ITC for MI-503 binding to menin, demonstrating binding affinity (K_d) and stoichiometry (N). (E) Crystal structure of MI-503 bound to menin. Protein is shown in ribbon representation and key menin residues involved in interactions with MI-503 are shown as sticks. MI-503 is shown in stick representation with colors corresponding to the atom type (green: carbons, dark blue: nitrogens, yellow: sulfur,

light blue: fluorine). Dashed lines represent hydrogen bonds between the ligand and protein. See also Figure S1 and Tables S1, S2 and S3.

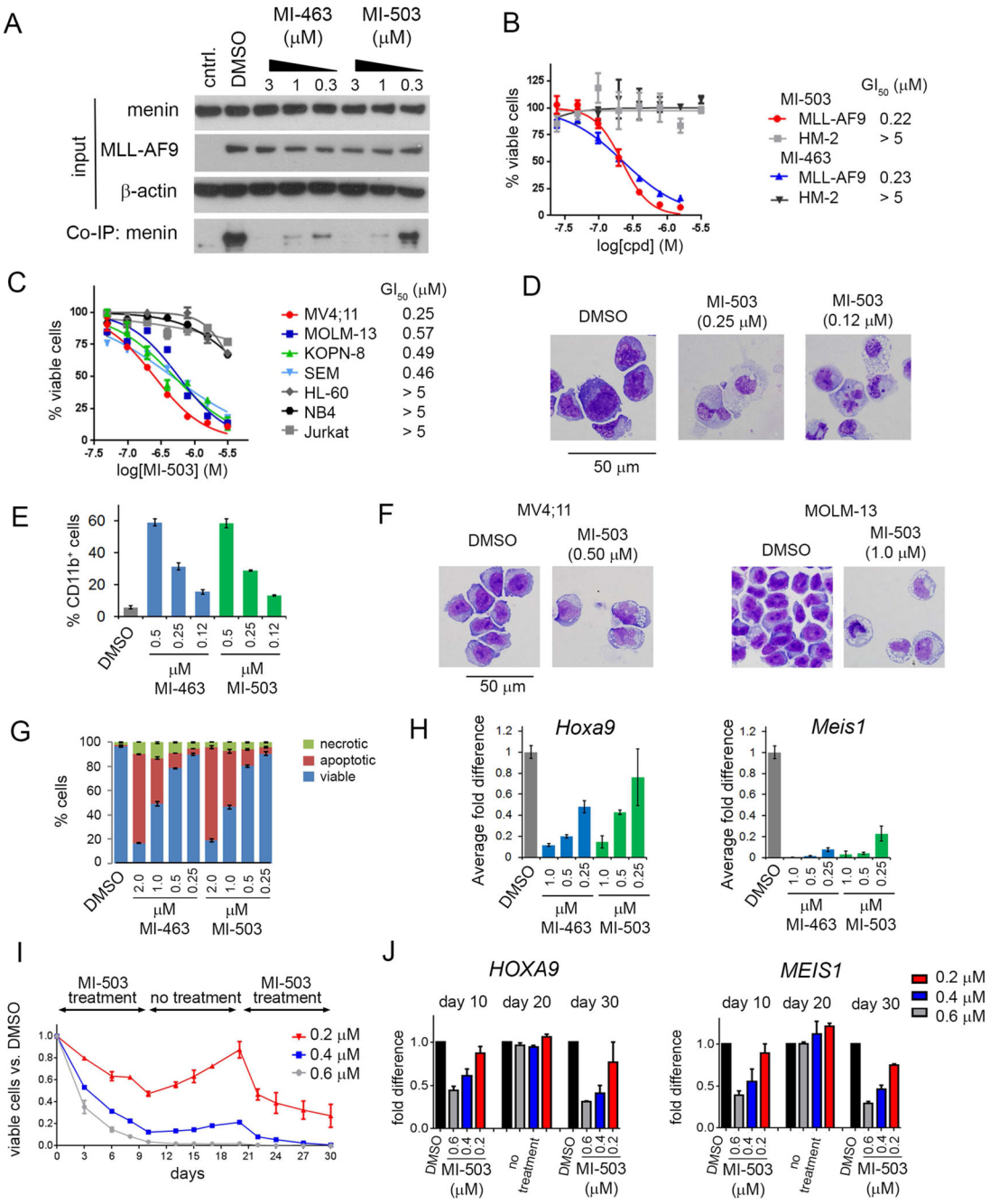

Figure 2. Activity of menin-MLL inhibitors in MLL leukemia cells

(A) Co-immunoprecipitation experiment in HEK293 cells transfected with MLL-AF9 upon treatment with DMSO, MI-463 and MI-503. Control (cntrl) represents an untransfected sample. (B) Titration curves from MTT cell viability assay after 7 days of treatment with MI-463 and MI-503 of MLL-AF9 and Hoxa9/Meis1 (HM-2) transformed murine bone marrow cells (BMCs); mean ± SD, n = 4. (C) Titration curves from MTT assay performed for 7 days of treatment of human MLL leukemia cell lines with MI-503: MV4;11 (MLL-AF4), MOLM-13 (MLL-AF9), KOPN-8 (MLL-ENL) and SEM (MLL-AF4) and control

AML cell lines without MLL translocations: HL-60, NB4 and Jurkat; mean ± SD, n = 4. (D) Wright-Giemsa-stained cytospins for MLL-AF9 transformed BMCs after 10 days of treatment with MI-503. (E) Quantification of CD11b expression in MLL-AF9 transformed BMCs treated for 7 days with MI-463 and MI-503 detected by flow cytometry; mean ± SD, n = 2. (F) Wright-Giemsa-stained cytospins for MV4;11 and MOLM-13 after 7 days of treatment with MI-503. (G) Apoptosis and cell death induced by MI-463 and MI-503 after 7 days of treatment in the MLL-AF9 BMC. Quantification of Annexin V and Propidium Iodide (PI) staining was detected by flow cytometry; mean ± SD, n = 2. (H) Quantitative real-time PCR performed in MLL-AF9 BMCs after 6 days of treatment with MI-463 and MI-503. Expression of *Hoxa9* and *Meis1* was normalized to β-actin and referenced to DMSO-treated cells; mean ± SD, n = 2. (I) Long term viability studies with different concentrations of MI-503 in MV4;11 cells. Cells were treated for 10 days, followed by 10 days of no treatment with subsequent 10 days of additional treatment. Viable cells were normalized to DMSO control. (J) Quantitative RT- PCR performed in MV4;11 cells upon treatment with MI-503 or DMSO at the end of each treatment or withdrawal phase (days 10, 20 and 30). Expression of *HOXA9* and *MEIS1* was normalized to 18S rRNA and referenced to DMSO-treated cells. Data in I and J represent mean values for duplicates ± SD. See also Figure S2.

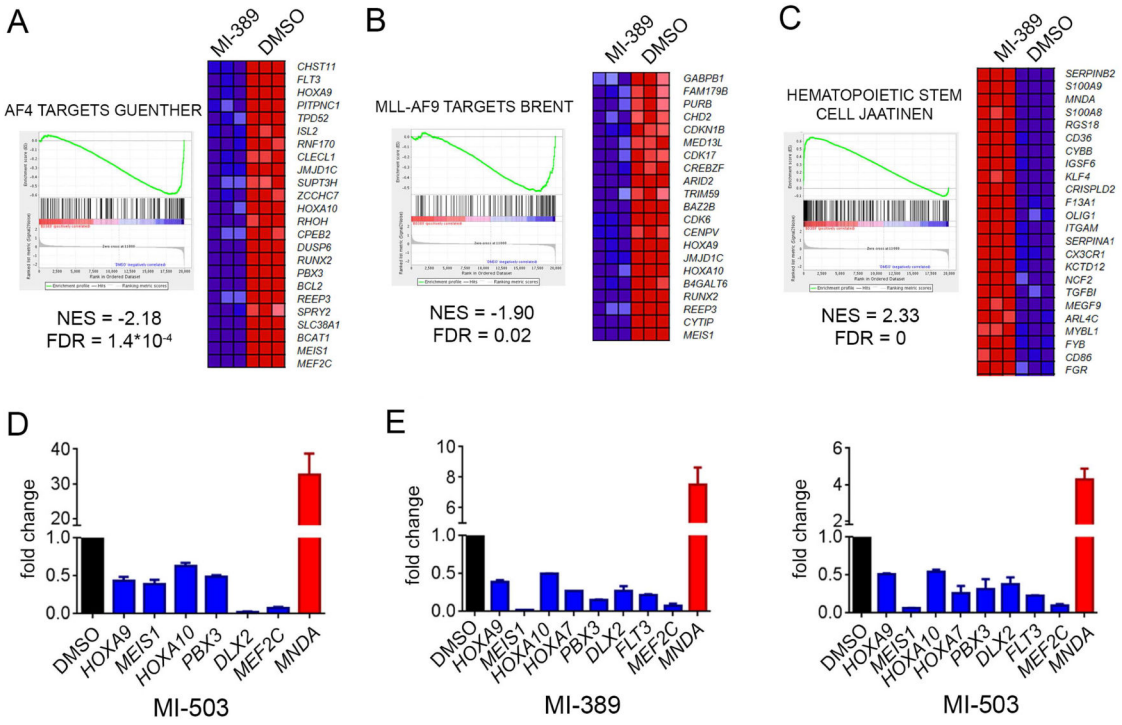

Figure 3. Effect of menin-MLL inhibitors on gene expression in MLL-rearranged human leukemia cells

(A, B) Gene Set Enrichment Analysis (GSEA) of genes downregulated upon treatment with MI-389 in MV4;11 cells as compared with genes bound by MLL-AF4 in human SEM cells (Guenther et al., 2008) (A) or MLL-AF9 targets (Bernt et al., 2011) (B). (C) GSEA of genes upregulated by MI-389 treatment of MV4;11 cells as compared with genes underexpressed in primitive hematopoietic progenitor cells (Jaatinen et al., 2006). The heat maps show genes comprising the leading edge of the GSEA plots. Red indicates high expression, blue indicates low expression. Triplicate samples were used for global gene expression studies. NES: Normalized Enrichment Score, FDR: False Discovery Rate. (D) Quantitative RT-PCR performed in MV4;11 cells after 10 days of treatment with 0.6 μM of MI-503. (E) Quantitative RT-PCR performed in MOLM-13 cells after 6 days of treatment with MI-389 (2 μM) or MI-503 (1 μM). Expression of genes in (D) and (E) was normalized to 18S rRNA and referenced to DMSO-treated cells. Data in (D) and (E) represent mean values for duplicates ± SD. See also Figure S3 and Table S4.

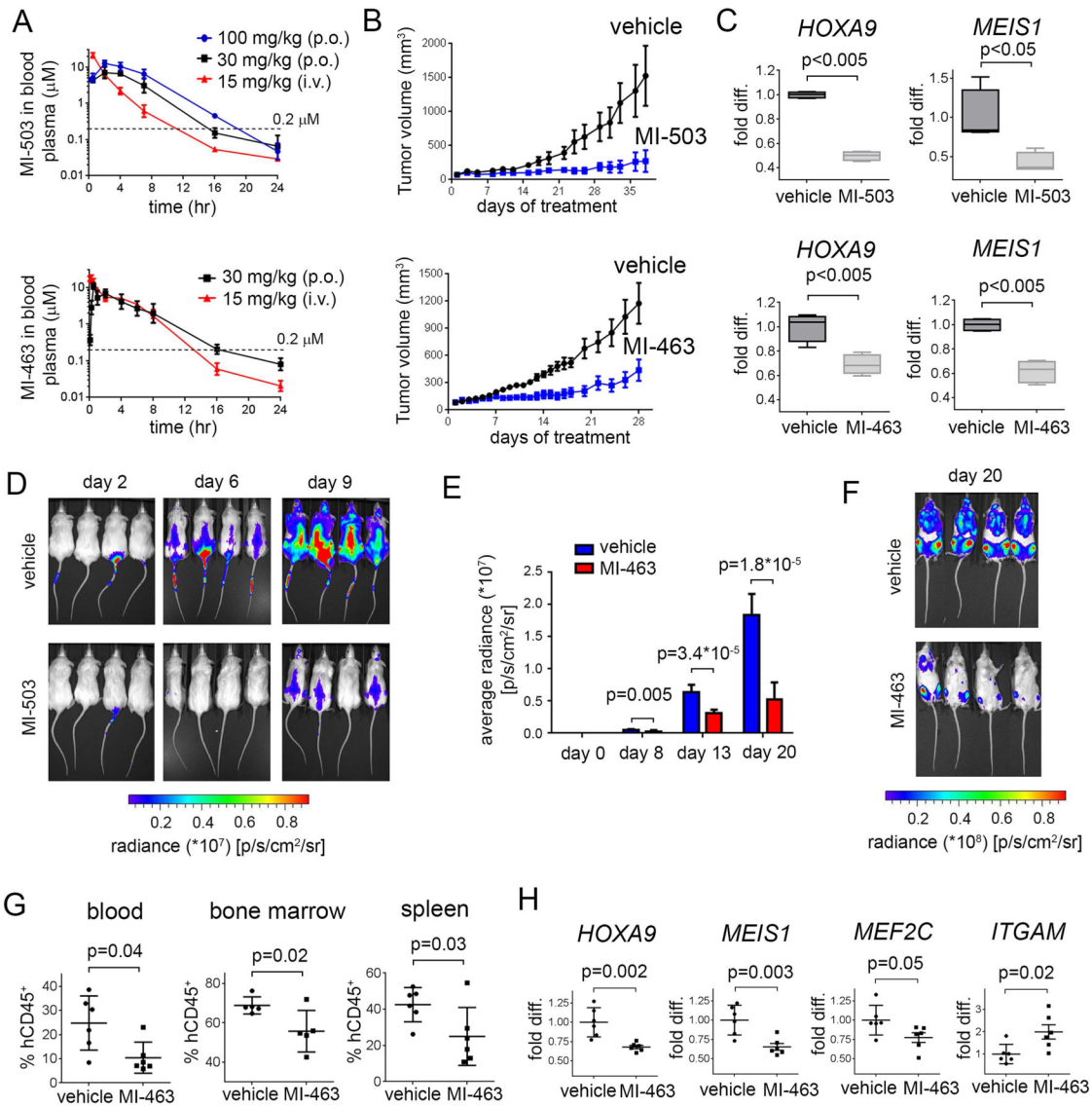

Figure 4. Menin-MLL inhibitors block hematological tumors in vivo, increase survival and reduce MLL leukemia tumor burden

(A) Pharmacokinetic studies in mice performed for MI-503 (top panel, mean ± SD, n = 2) and MI-463 (bottom panel, mean ± SD, n = 2) demonstrating blood concentration of the compounds after oral (p.o.) dose of 30 mg/kg or 100 mg/kg as well as intravenous (i.v.) administration at 15 mg/kg. (B) In vivo inhibition of the tumor growth by MI-503 (top panel) and MI-463 (bottom panel) after subcutaneous injection of 1×10^7 MV4;11 cells into BALB/c nude mice, n = 6 per group. Mice were treated once daily with MI-503 (60 mg/kg) or MI-463 (35 mg/kg) via i.p. ($p < 0.003$ for each compound). Error bars represent SEM. (C) Expression of *HOXA9* and *MIES1* measured by qRT-PCR of RNA extracted from tumor samples harvested at the end point of treatment with MI-503 (day 38, top panel) or MI-463 (day 28, bottom panel). *HOXA9* and *MEIS1* transcripts levels are normalized to the mean transcript level in tumors from the vehicle treated groups; n = 4 per group. Boxes represent the first and third quartiles, the line represents the median and the whiskers show the lowest

and the highest values. (D) Bioluminescent imaging of NSGS mice transplanted with MV4;11 human MLL leukemia cells expressing luciferase at the indicated days after initiation of treatment with MI-503 (60 mg/kg, twice daily every 12 hr, i.p.) or vehicle, n = 9 mice per group. (E) Quantification of bioluminescence imaging in NSG mice transplanted with luciferase-expressing MV4;11 cells at the indicated days after initiation of treatment with MI-463 (45 mg/kg, twice daily, p.o.) or vehicle, n = 6–7 mice per group. Error bars represent SEM. (F) Bioluminescence imaging of mice from panel (E) at the last day of treatment (day 20). (G) Flow cytometry quantification of human $CD45^+$ cells in blood, spleen and bone marrow samples harvested from NSG mice transplanted with MV4;11 cells after last treatment (day 20) with MI-463 or vehicle. Error bars represent SEM, n = 5–6. (H) Expression of *HOXA9*, *MIES1*, *MEF2C* and *ITGAM* measured by qRT-PCR of RNA extracted from spleen samples harvested after last treatment (day 20) with MI-463 or vehicle. Transcripts levels are normalized to GAPDH and referenced to the mean transcript level in vehicle treated group, which is set as 1 (n = 6 independent samples per group). Error bars represent SEM. See also Figure S4.

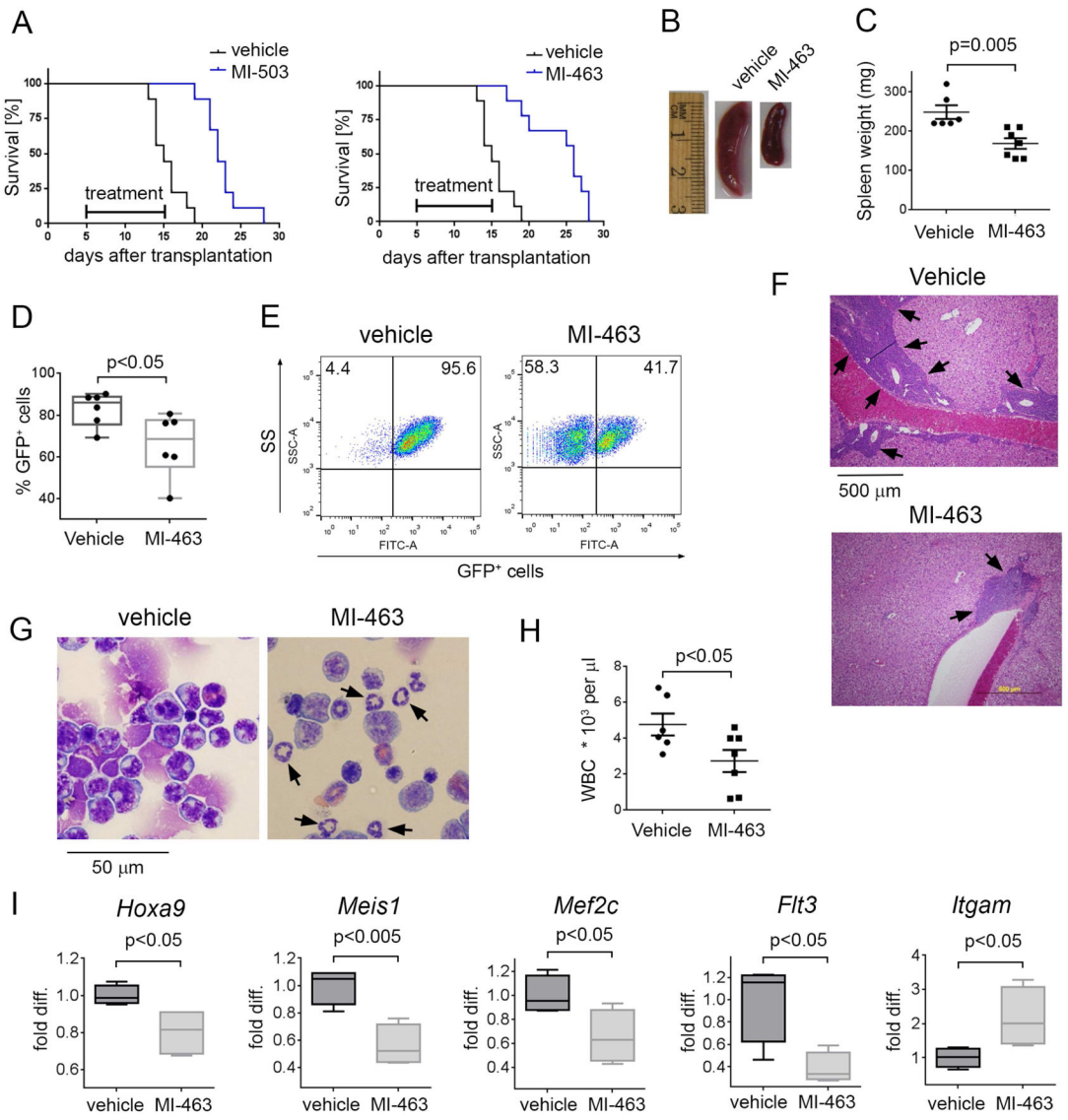

Figure 5. Treatment with menin-MLL inhibitor blocks progression of MLL leukemia in vivo

(A) Kaplan-Meier survival curves of vehicle and MI-503 or MI-463 treated C57BL/6 mice transplanted with 1×10^5 syngeneic MLL-AF9 leukemic cells isolated from primary recipient mice (n = 9 mice per group). Time of treatment is indicated on each graph. P values were calculated using Log-rank (Mantel-Cox) test, and are $p < 0.0001$ for each compound. (B) Representative photographs of the spleen from control and MI-463 treated (40 mg/kg, twice daily, p.o.) MLL-AF9 leukemia mice (n = 6–7 mice per group). Treatment was initiated 5 days after transplantation and continued for 10 days. Samples from all mice were collected one day after treatment was stopped. (C) Comparison of spleen weight for the MLL-AF9 leukemia mice treated with vehicle (n = 6) or MI-463 (n = 7), treatment as described in panel (B); mean ± SEM. (D) Quantification of leukemic blasts in bone marrow of MLL-AF9 leukemia mice upon treatment with MI-463 or vehicle (n = 6 mice per group) by flow cytometry analysis. GFP (Green Fluorescent Protein) is detected as a surrogate for MLL-AF9 expressed from the MigR1 vector, reflecting MLL-AF9 expressing leukemic

blasts. Boxes represent the first and third quartiles, the line represents the median and the whiskers show the lowest and the highest values. (E) Representative histograms from flow cytometry analysis of the leukemic blasts in bone marrow samples of the MLL-AF9 mice treated with vehicle or MI-463. SS – side scatter. (F) Histological sections of liver parenchyma from control and MI-463 treated mice. (G) Wright-Giemsa-stained cytospins for bone marrow samples isolated from MLL-AF9 mice treated with MI-463 and vehicle (treatment described in B). Bone marrow cells with neutrophil-like morphology in MI-463 treated mice are indicated by black arrows. (H) Treatment with MI-463 reduces white blood cell (WBC) level in the peripheral blood; mean ± SEM, n = 6. (I) Expression of *Hox9*, *Meis1*, *Mef2c*, *Flt3* and *Itgam* measured by qRT-PCR of RNA extracted from bone marrow samples harvested the next day after last treatment (treatment was continued for 10 days) with MI-463 or vehicle. Transcripts levels are normalized to β-actin and referenced to the mean transcript level in vehicle treated group, which is set as 1 (n = 4 replicates per group). Boxes represent the first and third quartiles, the line represents the median, and the whiskers show the lowest and the highest values. See also Figure S5.

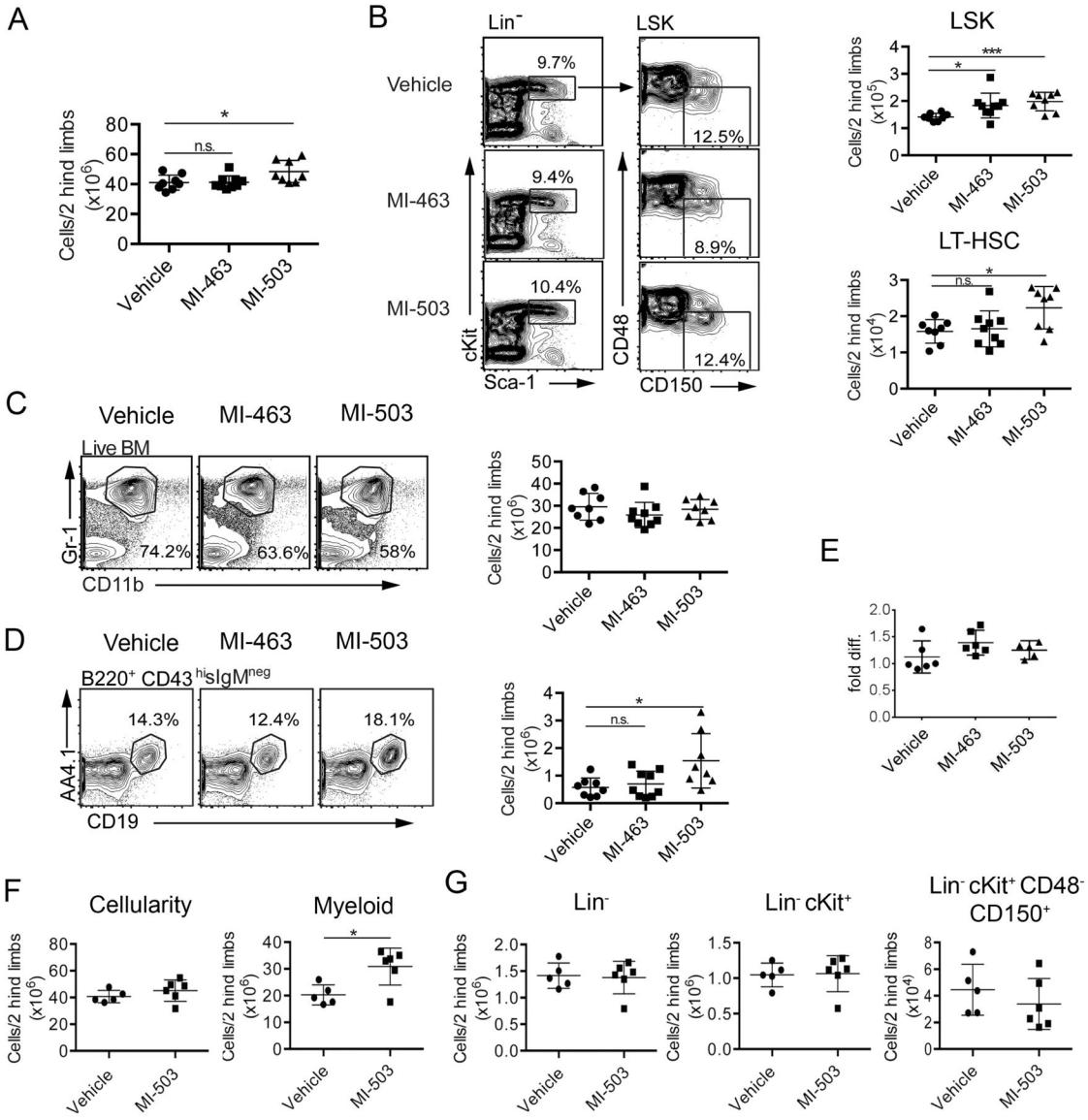

Figure 6. Pharmacologic inhibition of the menin-MLL interaction does not impair normal hematopoiesis in mice

(A) Analysis of bone marrow (BM) cellularity after 10 days of treatment of normal C57BL/6 mice with MI-463 (40 mg/kg), MI-503 (70 mg/kg) or vehicle control (twice daily via oral gavage; n = 8–9/group, mean ± SD). ns – not significant. (B) Representative histograms from flow cytometry analysis of hematopoietic stem and progenitor cells: LSK ($Lin^{-}Sca\text{-}1^{+}c\text{-}Kit^{+}$) and long-term repopulating cells (LT-HSC, defined as $Lin^{-}Sca\text{-}1^{+}c\text{-}Kit^{+}CD48^{-}CD150^{+}$), left panel. Right panel: quantification of LSK and LT-HSC cell frequency by flow cytometry (n = 8–9/group, mean +/− SD), *p<0.05, ***p<0.001 (treatment described in panel A). (C) Representative histograms (left panel) and quantification (right panel) from fIow cytometry analysis of mature myeloid cells in bone marrow (BM) samples isolated from mice treated with vehicle, MI-463 or MI-503 (n = 8–9/ group, mean ± SD); treatment described in panel (A). (D) Representative histograms (left

panel) and quantification (right panel) from flow cytometry analysis of BM pro-B cell populations ($B220^{+}CD43^{hi}sIgM^{neg}CD19^{+}AA4.1^{+}$) (n = 8–9/group, mean ± SD). *p<0.05. (E) Expression of *Hoxa9* measured by qRT-PCR of RNA extracted from LSK cells harvested after 10 days of treatment with MI-463, MI-503 or vehicle. Transcripts levels are normalized to *Hprt1* and referenced to the mean transcript level in vehicle treated group, which is set as 1 (n = 5–6 per group), mean ± SD. (F) Analysis of bone marrow cellularity and mature myeloid cells after 38 days of treatment with MI-503 (60 mg/kg, once daily, i.p.) or vehicle in the subcutaneous MV4;11 xenograft mice (BALB/c nude); mean ± SD, n = 5–6 per group. (G) Analysis of hematopoietic progenitor cells after 38 days of treatment with MI-503 (60 mg/kg, once daily, i.p., n = 5–6/group, mean ± SD). Analysis was performed in the subcutaneous MV4;11 xenograft mice (BALB/c nude), *p<0.05. See also Figure S6.

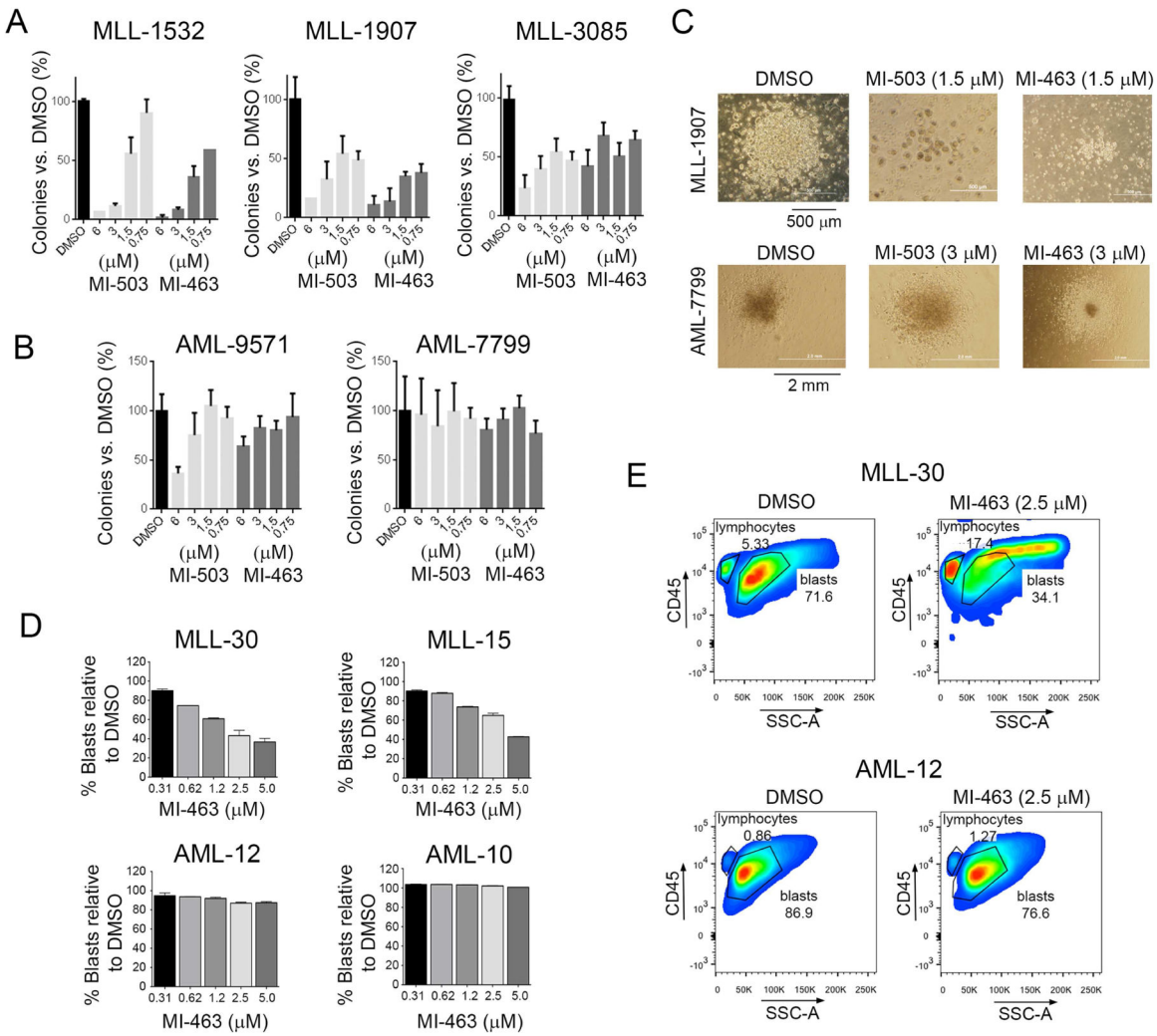

Figure 7. Menin-MLL inhibitors selectively kill MLL leukemia primary patient samples

(A, B) Colony counts for methylcellulose colony forming assay performed upon 14 days of treatment with MI-463 and MI-503 in primary patient samples with MLL leukemia (A) and in AML primary patient samples without MLL translocations (B). Colony counts are normalized to DMSO treated samples (mean ± SD, n= 2). (C) Pictures of colonies in one primary sample with MLL translocation (MLL-1907, top) and one AML primary sample without MLL translocation (AML-7799, bottom) treated as indicated. (D) Flow cytometry analysis of human $CD45^+$ cells upon 7 days of treatment of primary patient samples with MLL translocations (MLL-30, MLL-15) and without MLL translocations (AML-12, AML-10) with MI-463 or DMSO. Percentage of blasts in each sample is shown (mean ± SD, n = 2). (E) Histograms from flow cytometry analysis of blasts level ($hCD45^+$ cells) upon treatment of primary patient samples with MI-463 and DMSO. See also Figure S7.